JMEPEG (2009) 18:137–144
DOI: 10.1007/s11665-008-9255-z

1059-9495/$19.00

Microstructure and Mechanical Properties of AZ91 Alloys by Addition of Yttrium

Shou-Ren Wang, Pei-Quan Guo, Li-Ying Yang, and Yanjun Wang

(Submitted July 15, 2007; in revised form May 7, 2008)

Effects of yttrium (Y) on the microstructure and properties of as-cast Mg-Al-Zn (AZ91) alloys were studied. Y additions not only change the microstructure but also influence the mechanical properties of AZ91 alloy. AZ91 unmodified alloys under as-cast state indicate that eutectic phase $Mg_{17}Al_{12}$ is continuous and reticulated. Yttrium addition to AZ91 casting alloys has an important influence on the primary-phase and precipitation. When the Y content is 0.3 wt.%, no Y-containing compound was observed. When the Y content is 0.6 and 0.9 wt.%, Al_2Y phase formed in the alloy and the growth morphology of eutectic $Mg_{17}Al_{12}$ phase is modified. When the Y content is further increased to 1.2 wt.%, the Al_2Y phase becomes coarser and $Mg_{17}Al_{12}$ transforms into a cotton-shape structure. The results showed that Y can improve significantly as-cast microstructure of AZ91 alloys, refining $Mg_{17}Al_{12}$ phase and increasing in hardness and strength and decreasing in impact toughness and elongation.

Keywords Al_2Y, AZ91 alloy, $Mg_{17}Al_{12}$, modification, yttrium

1. Introduction

Magnesium alloys are attractive for automobile and aircraft engine applications because of their light-weight and high-specific strength. Recently, there has been significant increases in the usage of magnesium alloy for aerospace and automobile due to its low density, good damping characteristics, good thermal conductivity, and high-specific elastic modulus [Ref 1-3]. However, their poor performances at high temperature as strength, oxidation-resistance, and creep hamper the growth of their applications [Ref 4-7]. In order to improve elevated temperatures (ET) properties and to overcome the above disadvantages, a number of methods, such as hot extrusion [Ref 8], rapid solidification [Ref 9], directional solidification [Ref 10] and mechanical alloying [Ref 11], can be adopted to refine crystal particle, modify microstructure, and improve properties. But these processing methods may lead to the increase of production cost. One effective method is alloying. Mg is usually alloyed with Al, Ag, Mn, Zn, Si, Zr, and rare earth (RE) element. In particular, additions of RE element distinctly affect the microstructure and properties of Mg alloys [Ref 12-14]. In addition, additions of them can refine the microstructure and modify the morphology of precipitates. There are some literatures which discuss the effect of yttrium additions on the microstructure and properties of Mg alloy. The maximum solubility of yttrium in solid Mg is about 11 wt.% at 567 °C. M. Socjusz-Podosek [Ref 15] investigated the influence of yttrium (2 wt.%, 4 wt.%, and 6 wt.%) on the mechanical properties and microstructure of Mg-based alloys. Honghui Zou [Ref 16] reported that additions of yttrium element to the Mg-5 wt.% Zn-2 wt.% Al alloy lead to the formation of bacillary $Al_{11}Y_3$ phase and polygonal compound Al_2Y, and tensile properties of as-cast alloys at room temperature RT are improved substantially when yttrium content is above 1 wt.%. However, a high content of yttrium causes the occurrence of meta-stable precipitates, and that would increase alloy cost. From the engineering point of view, it is strongly recommended to reduce yttrium content without any deterioration of mechanical properties [Ref 17]. O.C. Jiang [Ref 17] discussed the modification of in situ formed Mg_2Si in Mg-Si alloys with 0.1, 0.4, 0.8, and 1.2 wt.% yttrium, respectively. AZ91 (AZ91) alloy is the most common magnesium casting alloy, it has good combination of castability, mechanical strength and ductility. The discontinuous precipitation usually occurs simultaneously and competitively with the continuous precipitation within the particle over a wider temperature range in AZ91 alloy. In particular, such a precipitate as $Mg_{17}Al_{12}$ often exhibits a continuous and reticulated morphology.

In the present works, microstructure of Mg-Al-Zn (AZ91) alloy by addition of yttrium has been discussed; the mechanical properties at RT and ET were investigated. The purpose of the study was to research the morphology, microstructure, and mechanical properties of modified alloy by addition of low contents of yttrium.

2. Experimental Procedure

Industrially pure Mg ingot (99.93 wt.% purity), Al ingot (99.95 wt.% purity), and Zn (99.85 wt.% purity) were used as starting materials to prepare Mg-Al-Zn alloy. All starting materials were melted in a stainless steel crucible (304) with an electric resistance furnace (SG-5-12) under protective Ar atmosphere (99.95% purity). After reaching the temperature of 780 °C and maintaining for 30 min, the desired amounts of

Shou-Ren Wang, Pei-Quan Guo, Li-Ying Yang, and **Yanjun Wang**, School of Mechanical Engineering, University of Jinan, Jinan 250022, China. Contact e-mail: sherman0158@tom.com.

Mg-10 wt.% Y master alloys were added in the crucible. Then, the melts were manually stirred for about 10 min using a graphite impeller to facilitate the incorporation and uniform distribution of yttrium in the metallic matrix. After the next 10 min, the melt temperature was lowered to 730 °C, held for 10 min and then the melts were poured into a steel mold being preheated at 300 °C. The dimension of specimen is Ø25 × 200 mm. The actual chemical compositions of fabricated alloy are shown in Table 1. Impurities as Mn, Si, Cu in specimen are introduced by master alloys. Grain sizes were measured using the linear-intercept method.

Microstructure and morphology were investigated by using scanning electron microscopy (SEM, Hitachi S-2500). Before observed the specimens were revealed by 0.5% Hydrofluoric Acid, etching time was about 20 s. Energy Dispersive Spectrometry analysis (EDS, OXFORD INCA) was performed to determine the phase's chemical constitution of the specimens. X-ray diffraction (XRD) investigations were carried out using a D/max-ra Advance diffractometer from Rigaku (Japan) with CuKa radiation selected by a secondary graphite monochromator. The step-scan mode with a step of 0.02 deg and a step-scan speed of 6 deg/min ($10^\circ \leq 2\theta \leq 80^\circ$) were used. Before grain size examination, the specimens were preheated to 350 °C for 16 h under the protection of Ar gas and then quenching. The linear-intercept method was employed to measure the grain size, eight of observed fields were selected and measured under the optical microscope. The tensile specimens were machined in accordance with procedures outlined in ASTM E8M-96. The sketch of tensile specimens and its geometry dimensions were shown in Fig. 1. There were no visible machining marks on the specimens and no evidence of fracture nucleation emanating from the specimen surface. The specimens were deformed to failure on a universal testing machine (Instron 5569) with initial strain rate of 0.005 min^{-1} and the strain was monitored by an extensometer with a gage length of 25 mm. Impact testing specimens were measured using JB3OA type impact testing machine, followed ASTM-A327M [Ref 18] specification by using un-notch specimens, as shown in Fig. 1b.

3. Results

3.1 Microstructure

According to the ternary phase diagram Mg-Al-Zn, the phases encountered in the diagram are α-Mg, β-$Mg_{17}Al_{12}$, ε-$MgZn_2$, and *T*-$Mg_{32}(Al,Zn)_{49}$ [Ref 19]. The as-cast microstructures of AZ91 alloy consist of primary α-Mg and eutectic β-$Mg_{17}Al_{12}$+α-Mg phase. The SEM micrographs of AZ91 alloys with different yttrium contents are shown in Fig. 2. The microstructure mainly shows dendrite morphology with the secondary phases distributed in interdendritic spacing and along grain boundaries. Figure 2a shows the SEM micrographs of as-cast alloys without addition of Y. As the second-phase, $Mg_{17}Al_{12}$ shows continuous and reticulated shape and distributes mainly at grain boundaries. XRD and EDS analyses (Fig. 3) reveal that the white phase is β-$Mg_{17}Al_{12}$ phase and the black is primary α phase. It can be validated by TEM and SADP micrographs which are shown in Fig 4. The electron diffraction pattern of this phase, after indexing, has been

Table 1 Actual chemical compositions of AZ91 alloys (wt.%)

No.	Y	Al	Zn	Mn	Si	Cu	Ni	Fe	Mg
a	0	8.6	0.7	0.25	<0.2	<0.05	<0.001	<0.0005	Balance
b	0.3	8.5	0.6	0.15	<0.2	<0.05	<0.001	<0.0005	Balance
c	0.6	8.5	0.5	0.23	<0.2	<0.05	<0.001	<0.0005	Balance
d	0.9	8.6	0.6	0.24	<0.2	<0.05	<0.001	<0.0005	Balance
e	1.2	8.8	0.7	0.19	<0.2	<0.05	<0.001	<0.0005	Balance
f	1.5	8.7	0.4	0.15	<0.2	<0.05	<0.001	<0.0005	Balance

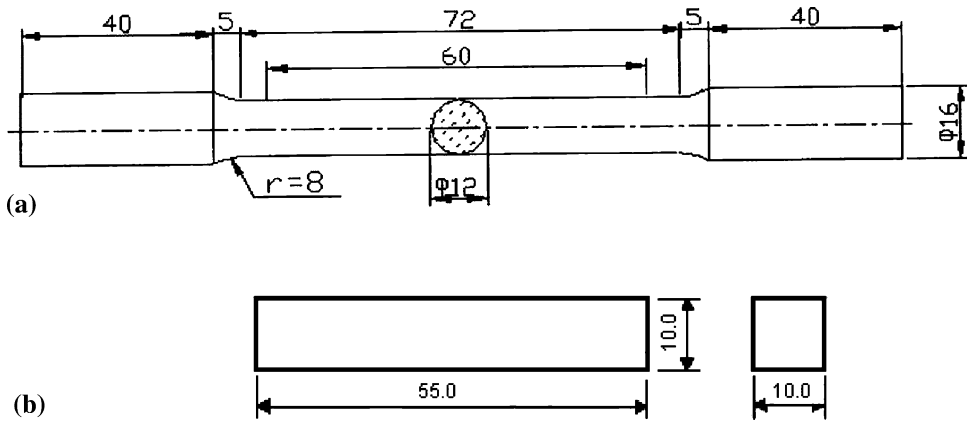

Fig. 1 The sketch of specimens and its geometry dimensions (a) Tensile specimens. (b) Impact-testing specimen

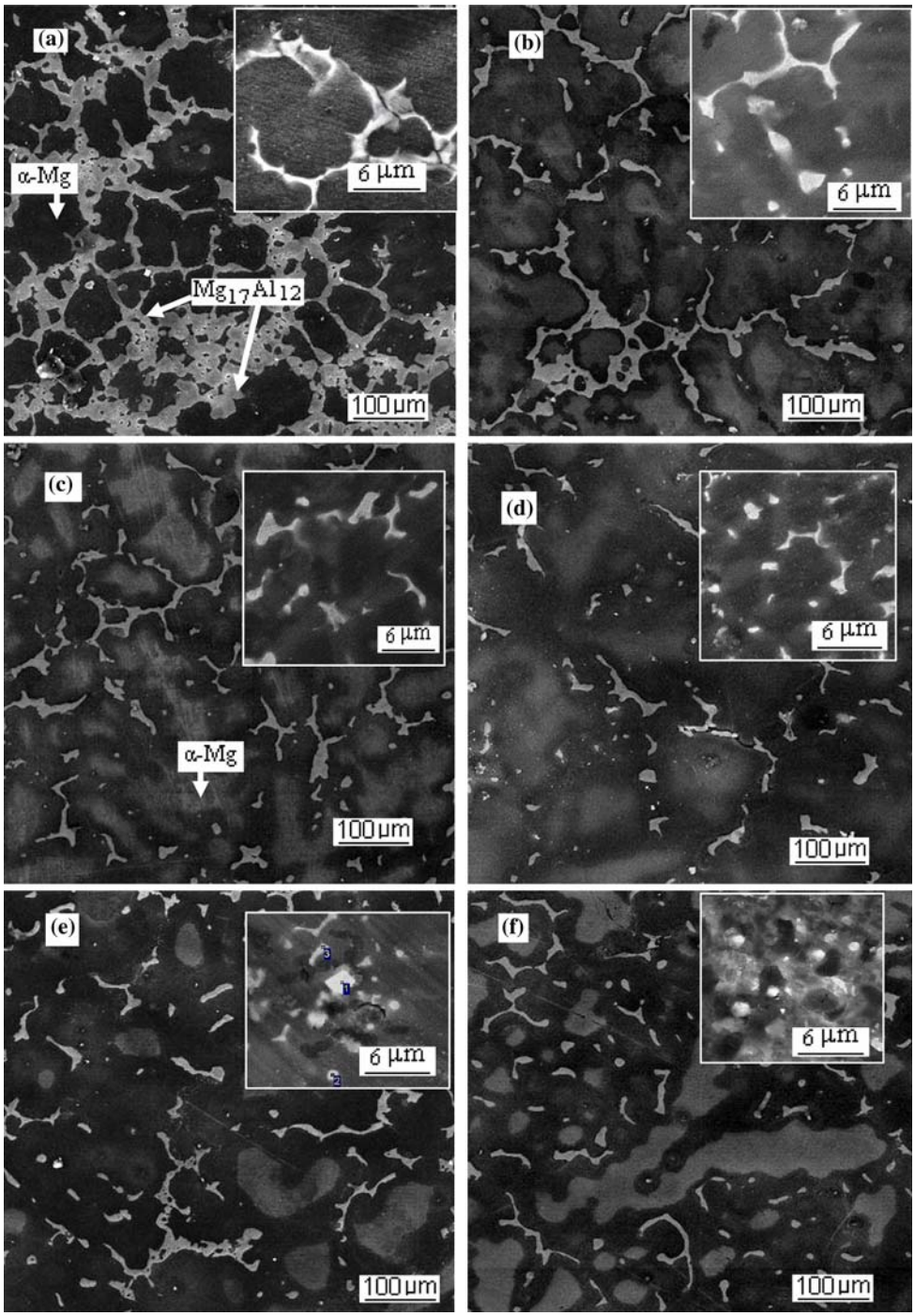

Fig. 2 SEM micrographs of Mg-Al-Zn as-cast alloys with different yttrium content. (a) without Y; (b) 0.3 wt.% Y; (c) 0.6 wt.% Y; (d) 0.9 wt.% Y; (e) 1.2 wt.% Y; (f) 1.5 wt.% Y

identified as $Mg_{17}Al_{12}$ of the structural type $A1_2$ with the lattice parameter as a = 1.056 nm.

Figure 2b-f shows the SEM microstructures of the as-cast alloys by additions of Y as 0.3, 0.6, 0.9, 1.2, and 1.5 wt.%, respectively. It is shown that the microtopography and structure of alloys were changed and modified by adding Y. Figure 5 shows the metallographic structure of AZ91 as-cast alloys with different yttrium contents. By adding Y, the amount of β $Mg_{17}Al_{12}$ is reduced and microstructure of that is refined. With the increases of Y contents the grain sizes of β phase turn smaller. Eutectic $Mg_{17}Al_{12}$ phase turns to discontinuous, more and more disperse phases occur with the increase of yttrium content.

In addition, the matrix phase is refined owing to the addition of Y; this can be shown in Fig. 6. Grain size of matrix phase is average 95 μm without Y addition and is average 55 μm with 0.9% Y after solute treatment (T4) measured by linear-intercept method. Distinctly, additions of Y in AZ91 alloys result in the modification of as-cast structure and grain size changes of both matrix grain and precipitates.

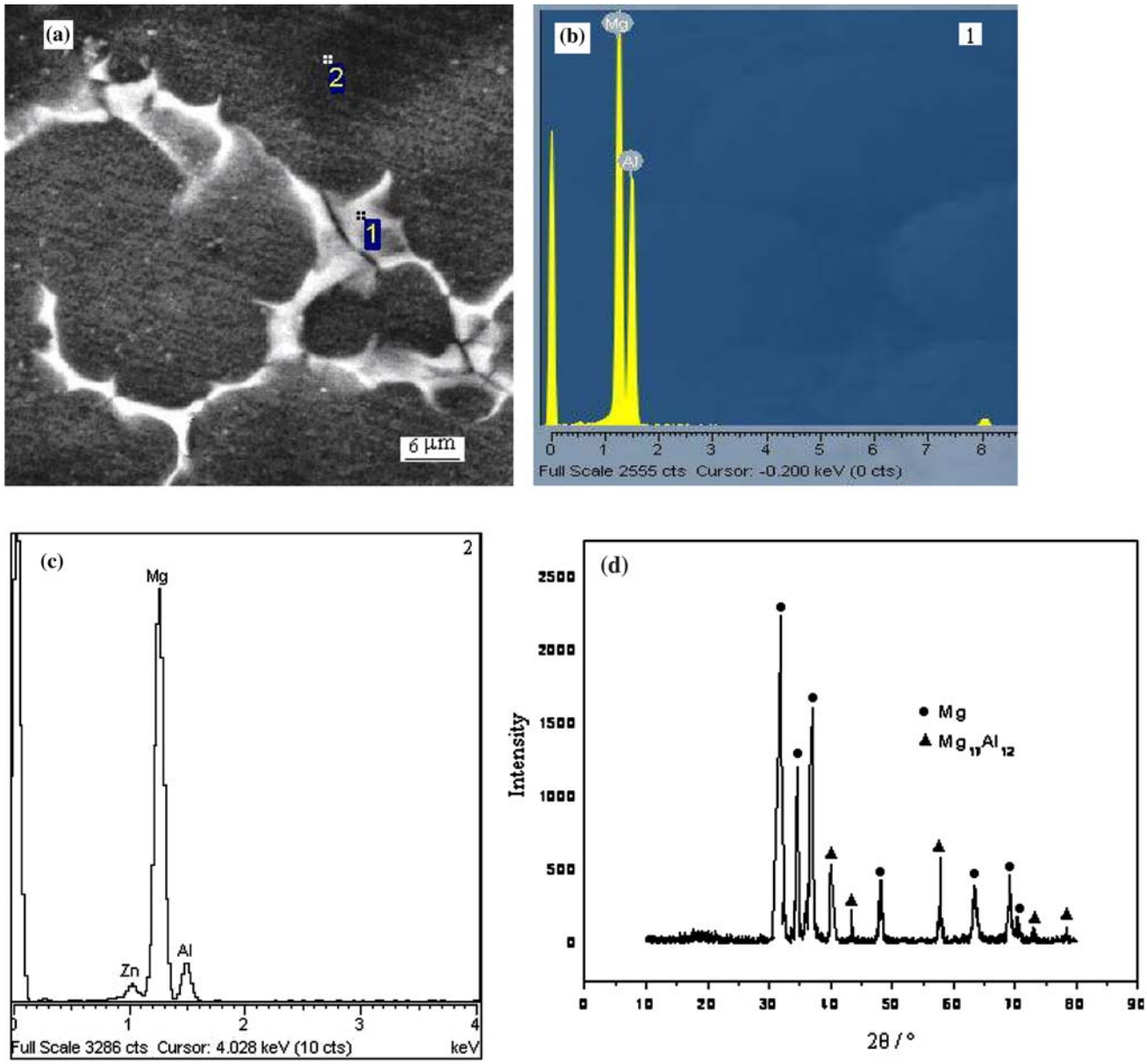

Fig. 3 SEM micrograph, results of the micro analyses of chemical composition by means of EDS and XRD pattern of AZ91 alloy without Y addition. (a) SEM; (b) 1 point EDS; (c) 2 point EDS; (d) XRD

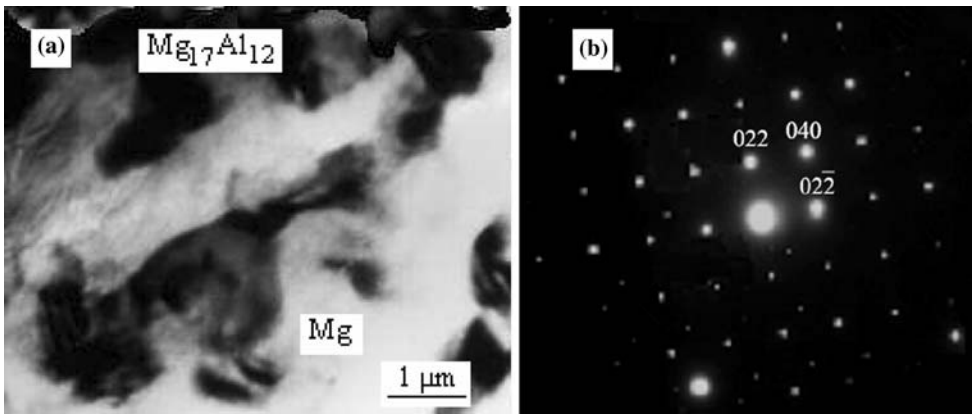

Fig. 4 TEM micrograph of AZ91 alloy and SADP pattern of eutectic phase. (a) TEM micrograph; (b) SADP pattern

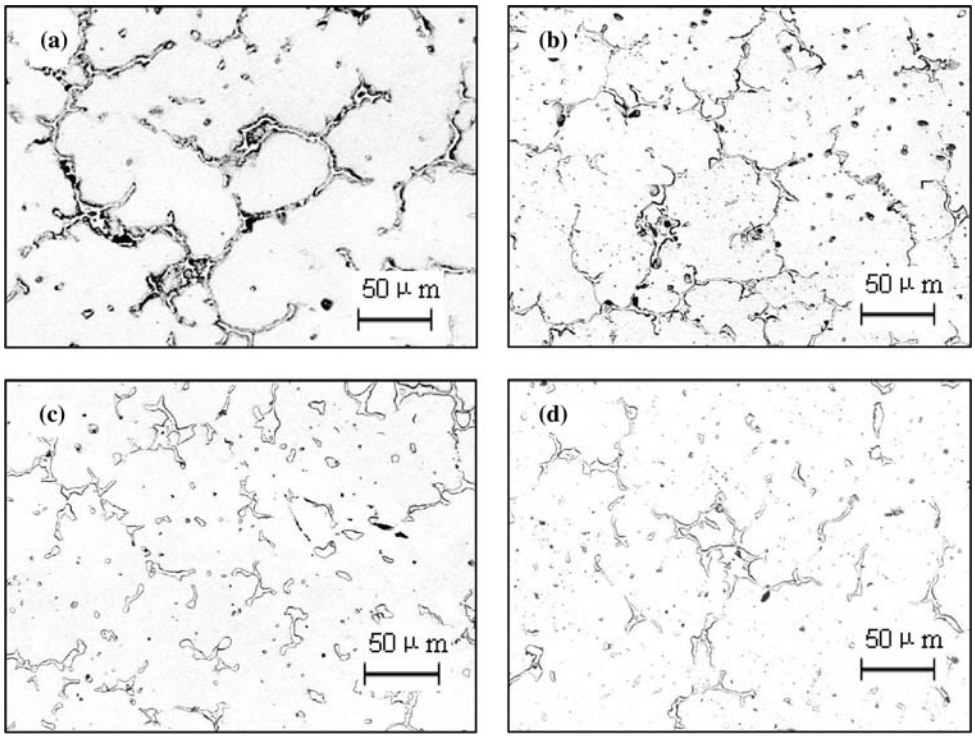

Fig. 5 Metallographic structure of AZ91 as-cast alloys with different yttrium contents. (a) Without Y; (b) 0.3 wt.% Y; (c) 0.6 wt.% Y; (d) 0.9 wt.% Y

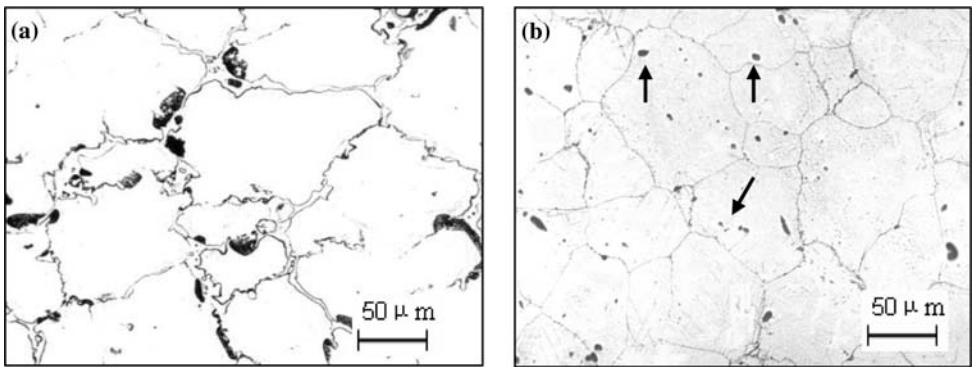

Fig. 6 Metallographic structure of AZ91 as-cast alloys after solute treatment (T4) (a) Without Y; (b) 0.9 wt.% Y

Meanwhile, there are more precipitate particles dispersing in the grains of Y-containing alloys. Figure 7 shows that the Y-containing phase is verified as Al_2Y ($2Al + Y = Al_2Y$) by XRD. This can be further tested by the TEM and SADP shown in Fig. 8. The corresponding electron diffraction patterns of this phase has been identified as Al_2Y of C15 (Cu_2Mg) structural type with lattice parameter $a = 0.786$ nm. Once Y content exceeds 0.9 wt.%, Al_2Y phase particles become more and more coarsening. Owing to the relatively high solubility of Y in Mg alloy (maximum solubility is 11 wt.% at 567 °C), a small amount of yttrium addition cannot form any Y-containing compound [Ref 20, 21]. However, owing to the existence of adequate amount of yttrium content and adequate content of Al in front of liquid-solid interface, Y atoms are very active in reaction with Al forming Y-Al compound. After homogenization treatment (Fig. 6), $Mg_{17}Al_{12}$ phases almost disappear. They gradually dissolve into α-Mg matrix and the amount of the second-phase decreases sharply. Due to the high melting point and the ET stability of Al_2Y particles (arrows in Fig. 6b), they are almost not dissolved in the α-Mg matrix and remain the original shape all the same time.

3.2 Mechanical Properties

It is well known that the mechanical properties of AZ91 alloy are strongly influenced by their microstructures. Some microstructural features which can influence the mechanical properties of alloy are grain size, dendrite arm spacing, volume fraction, and distribution of secondary phases or eutectic structures, and also interface characteristic between different phases [Ref 22]. Figure 9 shows the 0.2% yield strength (0.2%YS) and ultimate tensile strength (UTS) at RT. The strength of AZ91-Y alloy, both 0.2%YS and UTS at RT, was higher than the AZ91 alloy. Therefore, there are increases of 0.2%YS and UTS at RT with the increases of yttrium contents. When yttrium contents attain 0.6-0.9%, there are largest

strength not only 0.2%YS but also UTS. Once yttrium contents exceed 0.9%, decreases trend occurs (Fig. 9).

0.2%YS and UTS at ET as 200 °C are also shown in Fig. 9. The strength of AZ91-Y alloy, both 0.2%YS and UTS at ET, were higher than that of AZ91 alloy. This increase is ascribed to the following: (i) precipitation hardening, (ii) solution strengthening, (iii) changes of grain size of matrix grains and of the size of the precipitates, and (iv) dislocation creep with dispersion-strengthening.

Figure 10 shows the impact toughness and elongation at RT with different content of Y. Impact toughness and elongation at RT decrease gradually with the increasing of Y content, which is ascribed to the following reason as (i) precipitation hardening and (ii) solution strengthening.

4. Discussion

The reasons why additions of Y into the AZ91 alloy greatly affect the microstructures of as-cast alloy are as follows.

Al_2Y is hard to act as nucleating core of Mg due to its cubic structure and large lattice parameter ($a = 0.786 \times 10^{-9}$ m [Ref 23]). The melt point of Al_2Y is 1485 °C [Ref 15] and the crystallizing temperature of Al_2Y (980 °C) is higher than eutectic reaction temperature (L450 ° C α (Mg) + $Mg_{17}Al_{12}$). So, Al_2Y will preferentially form and concentrate at the front

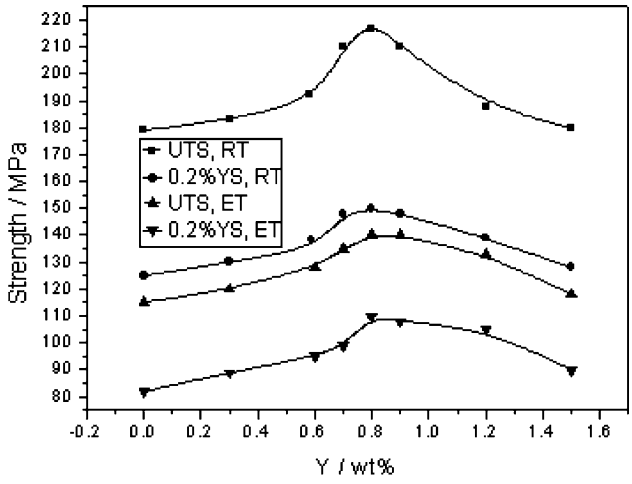

Fig. 9 Strength of AZ91 alloy with increasing of Y addition

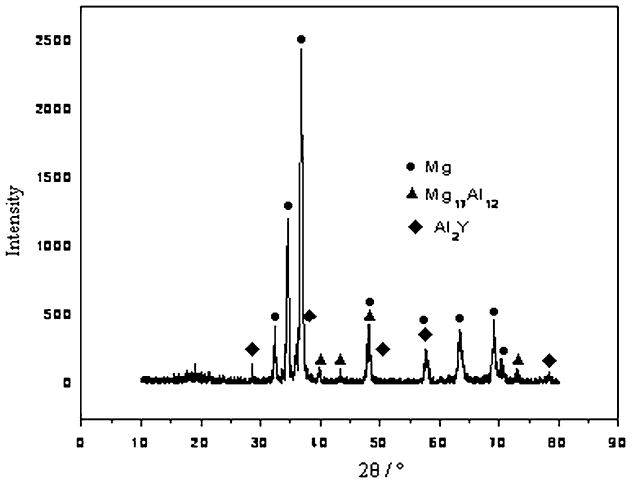

Fig. 7 XRD analyses of 1.2%Y in AZ91alloy

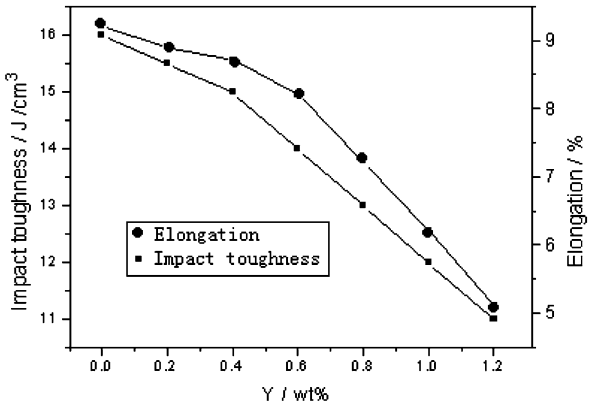

Fig. 10 Elongation and impact toughness of AZ91 alloy with increasing of Y addition

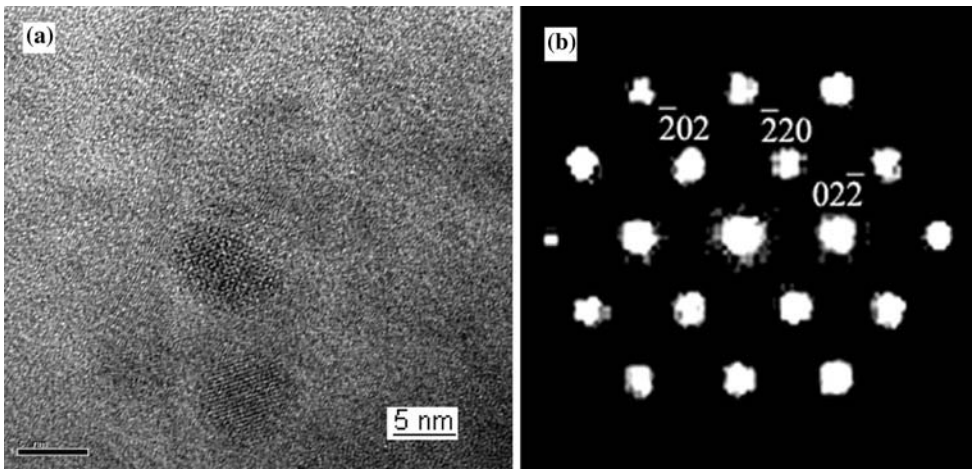

Fig. 8 TEM and SADP of Al_2Y phase (a) TEM; (b) SADP

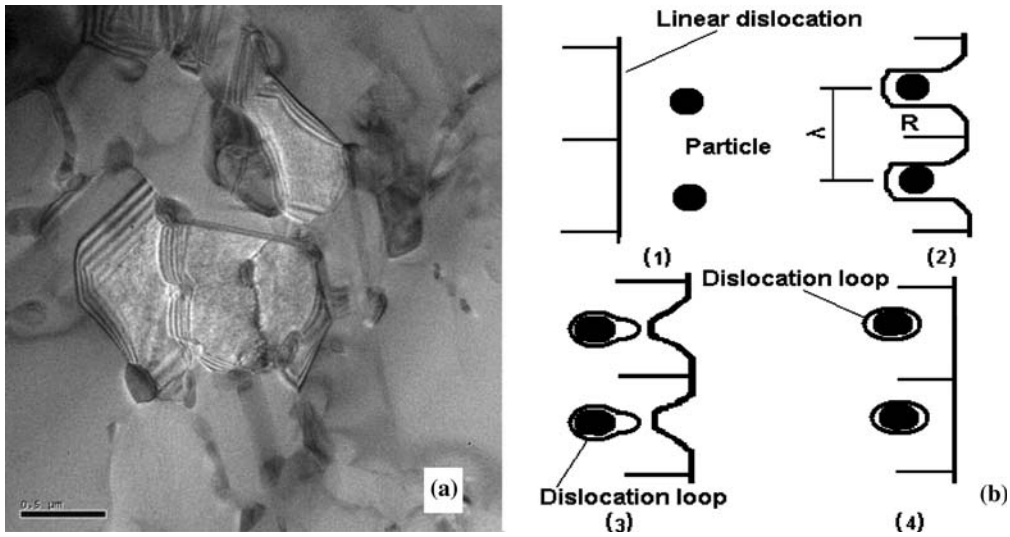

Fig. 11 Screw dislocation distribution and Orowan strengthening mechanism (a) Screw dislocation strengthening; (b) Orowan strengthening

edge of α-Mg phase. Thus, constitutional under-cooling appears ahead of the solid-liquid interface [Ref 24]. This driven power promotes the nucleation in the under-cooling zone. Meanwhile, the concentration of solute atoms at the solid-liquid interface can restrict the grain growth of primary and eutectic phase. Due to the slowly diffusion of solute atoms at the solid-liquid interface, grain growth is too slow before solidification. So, as-cast microstructure can be refined by the Y addition.

The improvement of mechanical properties is attributed to the conjoint influence of the following factors: (i) The effective transfer of stress from the soft magnesium alloy metal matrix to the reinforcing Al_2Y particulates resulting in the increases of strength (load-bearing strengthening); (ii) the stable Al_2Y phases are the barrier for the slip of dislocation, and cause more dislocations concentrate around it (enhanced screw dislocation density strengthening); and (iii) Orowan strengthening which is shown in Fig. 11. Indeed, with the increases of volume fraction of Y, both Orowan strengthening effect and enhanced dislocation density strengthening effect are found to play a significant role in AZ91-Y alloys.

The decreases (Y content exceed 0.9%) are ascribed to the following (i) preferential growth of Al_2Y phase formed large block crystal, (ii) the coarse Al_2Y phase particles result in the formation of micro-cracks and the flaws propagation, and (iii) large amount of Al_2Y lead to the un-symmetrical chemical composition and non-homogeneous microstructure.

5. Conclusions

(1) Eutectic $Mg_{17}Al_{12}$ phase in as-cast AZ91 alloys exhibits continuous and reticulated microstructure. The AZ91 alloys with variable Y contents all contain a phase of Al_2Y. Appropriate Y content refines the microstructures of as-cast alloys. Exceeding the amount of Y to more than 0.9% should lead to a coarsening of the grain structure. The optimal yttrium content in AZ91 alloy is proved to be about 0.9 wt.%, once exceeding this value would lead to the drops of tensile strength.

(2) Yttrium can improve significantly the strength of AZ91 alloys not only at RT but also at ET. The increases attribute to three strengthening mechanism: load-bearing, enhanced location density, and Orowan strengthening.

Acknowledgments

This work was supported by Science and Technology Project of Educational Committee (J07YA18) and Programs for Science and Technology Development of Shandong Province (2007ZG 10004013). Part of this research was done at the Institute of Materials Science of University of Jinan and school of Mechanical Engineering of University of Jinan. The authors owe a debt of gratitude to the technical staff of institutions for their help.

References

1. X.Y. Fand, D.Q. Yi, B. Wang, W.H. Luo, and W. Gu, Effect of Yttrium on Microstructures and Mechanical Properties of Hot Rolled AZ61 Wrought Magnesium Alloy, *Trans. Nonferrous Met. China*, 2006, **16**, p 1053–1058
2. B.L. Mordike and T. Ebert, Magnesium: Properties-Applications-Potential, *Mater. Sci. Eng. A*, 2001, **302**, p 37–45
3. Y. Kojima, Platform Science and Technology for Advanced Magnesium Alloys, *Mater. Sci. Forum*, 2000, **3**, p 350–351
4. Z. Koren, H. Rosenson, E.M. Gutman, Y.B. Unigovski, and A. Eliezer, Development of Semisolid Casting for AZ91 and AM50 Magnesium Alloys, *J. Light Met.*, 2002, **5**, p 81–87
5. T. Sumitomo, C.H. Caceres, and M. Veidt, The Elastic Modulus of Cast Mg–Al–Zn Alloys, *J. Light Met.*, 2002, **2**, p 49–56
6. G.Y. Yuan, M.P. Liu, W.J. Ding, and I. Akihisa, Microstructure and Mechanical Properties of Mg–Zn–Si-Based Alloys, *Mater. Sci. Eng. A*, 2003, **9**(25), p 314–320
7. M.T. Perez-Prado and O.A. Ruano, Texture Evolution During Grain Growth in Annealed MG AZ61 Alloy, *Scr. Mater.*, 2003, **1**, p 59–64
8. S.F. Hassan, K.F. Ho, and M. Gupta, Increasing Elastic Modulus, Strength and CTE of AZ91 by Reinforcing Pure Magnesium with Elemental Copper, *Mater. Lett.*, 2004, **6**, p 2143–2146
9. Y. Shin-ichi, K. Hyang-Yeon, K. Hisamichi, I. Akihisa, and A. Yoshiaki, Electrode Properties of Rapidly Solidified $Mg_{67}Ni_{23}Pd_{10}$ Amorphous Alloy, *J. Alloy. Compd.*, 2002, **12**(16), p 239–243
10. S. Gang, O. Keyna, C. Brian, W. John, and H. Richard, Growth Related Metastable Phase Selection in a 6xxx Series Wrought Al Alloy, *Mater. Sci. Eng. A*, 2001, **5**(31), p 612–616
11. L. Lu, M.O. Lai, and M.L. Hoe, Formation of Nanocrystalline Mg_2Si and Mg_2Si Dispersion Strengthened Mg-Al Alloy by Mechanical Alloying, *Nat. Mater.*, 1998, **4**, p 551–563

12. H.Z. Chi, C.P. Chen, L.X. Chen, and Q.D. Wang, Hydriding Properties of $La_2Mg_{16}Ni$ alloy Prepared by Mechanical Milling in Benzene, *J. Alloy. Compd.*, 2003, **10**, p 312–315
13. D.X. Zhao, Y.H. Liu, D.Z. Shen, J.Y. Zhang, Y.M. Lu, and X.W. Fan, The Dependence of Emission Spectra of Rare Earth Ion on the Band-Gap Energy of $Mg_xZn_{1-x}O$ Alloy, *J. Cryst. Growth*, 2003, **2**, p 163–166
14. Q.D. Wang, Y.Z. Lu, X.Q. Zeng, W.J. Ding, Y.P. Zhu, Q.H. Li, and J. Lan, Study on the Fluidity of AZ91+xRE Magnesium Alloy, *Mater. Sci. Eng. A*, 1999, **11**, p 109–115
15. M. Socjusz-Podosek and L. Litynska, Effect of Yttrium on Structure and Mechanical Properties of Mg Alloys, *Mater. Chem. Phys.*, 2003, **80**, p 472–475
16. H.H. Zou, X.Q. Zeng, C.Q. Zhai, and W.J. Ding, The Effects of Yttrium Element on Microstructure and Mechanical Properties of Mg–5 wt.% Zn–2 wt.% Al Alloy, *Mater. Sci. Eng. A*, 2005, **402**, p 142–148
17. O.C. Jiang, H.Y. Wang, Y. Wang, B.X. Ma, and J.G. Wang, Modification of Mg_2Si in Mg-Si Alloys with Yttrium, *Mater. Sci. Eng. A*, 2005, **392**, p 130–135
18. ASTM A327-91, Standard Test Methods for Impact Testing of Cast Irons (Metric), 1996
19. P. Liang, T. Tarfa, L.A. Robinson, S. Wagner, P. Ochin, M.G. Harmelin, H.J. Seifert, H.J. Lukas, and F. Aldinger, Experimental Investigation and Thermodynamic Calculation of the Al-Mg-Zn System, *Thermochim. Acta.*, 1998, **314**, p 87–110
20. F. Von Buch, J. Lietzau, and B.L. Mordike, Development of Mg_2Sc_2Mn Alloys, *Mater. Sci. Eng. A*, 1999, **263**, p 1–7
21. B.L. Mordike, Creep-Resistant Magnesium Alloys, *Mater. Sci. Eng. A*, 2002, **324**, p 103–112
22. H. Cao and M. Wessen, Effect of Microstructure on Mechanical Properties of As-Cast Mg-Al Alloys, *Metall. Mater. Trans. A*, 2004, **35**, p 309–312
23. M.D. Nave, A.K. Dahle, and D.H. Stjohn, Eutectic Growth Morphologies in Magnesium-Aluminum Alloys, *Magnesium Tech.*, 2000, TMS, p 233–242
24. Z.P. Luo, D.Y. Song, and S.Q. Zhang, Strengthening Effects of Rare Earths on Wrought Mg-Zn-Zr-RE Alloys, *J. Alloy. Compd.*, 1995, **230**, p 109–114